6th International Conference on CFD in Oil & Gas, Metallurgical and Process Industries
SINTEF/NTNU, Trondheim NORWAY *CFD08-38*
10-12 June 2008

A DISCRETE ELEMENT STUDY OF MOISTURE DEPENDENT PARTICLE-PARTICLE INTERACTION DURING GRANULATION IN A SPOUT FLUIDIZED BED

Maureen S. van Buijtenen[1] , Niels G. Deen[1]*, Stefan Heinrich[2], Sergiy Antonyuk[2] and J.A.M. Kuipers[1]

[1] University of Twente, Faculty of Science and Technology, Institute for Mechanics Processes and Control Twente
PO Box 217, Enschede, 7500 AE, The Netherlands

[2] Otto-von-Guericke-University Magdeburg, Faculty of Process and Systems Engineering
PO Box 4120, 39106 Magdeburg, Germany

* E-mail: N.G.Deen@utwente.nl

ABSTRACT

Spout fluidized beds find widespread application in the process industry in granulation processes, in which efficient contacting between large particles, droplets and gas is of paramount importance. However, detailed understanding of the complex behavior of these systems is lacking. In this paper we study the effect of the inter-particle interaction on the bed dynamics, by investigating the bed height, pressure drop and vertical particle velocity as function of the variable restitution coefficient, which varies in time and space as function of the moisture content due to the particle-droplet interaction. This is done computationally, by using the extended discrete element model (DEM) which describes the dynamics of the continuous gas-phase and the discrete particles and droplets. The objective of this work is to gain insight in the effect of the variable restitution coefficient on the flow behavior of spout fluidized beds at different flow regimes using DEM. The three flow regimes comprise the intermediate / spout-fluidization regime (B1), spouting-with-aeration regime (B2) and the jet-in-fluidized-bed regime (B3). The simulation results with variable restitution coefficients were compared to simulations with constant restitution coefficients reported by Van Buijtenen et al. (2007). The trend of increasing average bed height with decreasing restitution coefficient is also valid for the variable restitution coefficient. However, the average bed height is larger for the variable restitution coefficient for all flow regimes. This is also observed for the pressure drop, showing a lower value compared to the constant restitution coefficient. These results suggest a significant influence of the variable restitution coefficient on the bed dynamics, since the variable restitution coefficient provides regions in the bed with particles having different collision properties. The presence of these distinctive regions causes different behavior of the bed dynamics, which is also shown in the time-averaged vertical particle velocity. The velocity in the spout region for the variable restitution coefficient is lower than for the constant restitution coefficient for case B1 and B2. However, for case B3 these regions are less pronounced, due to the larger mixing capacity caused by the larger interaction between the spout channel and the bubbles in the annulus region. As a result, the particle velocity for the variable restitution coefficient complies with the particle velocity for the constant restitution coefficient.
These findings reveal the significant impact of the influence of the variable restitution coefficient on the dynamics of the bed, which is clearly different compared to the constant restitution coefficient. This is due to the presence of distinctive regions with different restitution coefficient, which can only be simulated when the dependency of the moisture content on the restitution coefficient is accounted for.
Currently, only the wetting process on the particles has been simulated without evaporation and crystallization of the deposited granulate solution, which are phenomena that are very important in the granulation process. It is therefore desirable to further improve the discrete element model, by solving mass and energy balances for the particles and the gas phase.

Keywords: Granulation, discrete element model, spout fluidized beds, restitution coefficient.

NOMENCLATURE

d	diameter [m]
D	distribution function [-]
e_n	coefficient of normal restitution [-]
$e_{n,p}$	variable coefficient of normal restitution [-]
$e_{n,p0}$	initial variable coefficient of normal restitution [-]
$e_{n,psat}$	variable coefficient of normal restitution of a saturated particle [-]
$\mathbf{g}$	gravitational acceleration [m/s^2]
$F_{a\leftrightarrow b}$	force due to particle-particle interaction [N]
$\langle H_{bed} \rangle$	time-averaged bed height [m]
$\mathbf{I}$	unit vector [-]
k_n	spring stiffness [N/m]
m_p	particle mass [kg]
m_d	droplet mass [kg]
N_p	number of particles [-]
$\dot{N}_{drop}$	rate of injection droplets [drops/s]
N_t	number of time steps [-]
N_x	number of gridcells x-direction [-]
N_y	number of gridcells y-direction [-]
N_z	number of gridcells z-direction [-]
N_{walls}	number of system walls [-]
p	pressure [Pa]
$\langle \mathbf{p} \rangle$	time-averaged pressure drop [Pa]
$\mathbf{r}$	position [m]
Re_p	particle Reynolds number [-]
$\mathbf{S}_p$	particle drag sink term [N/m^3]
t	time [s]
Dt	time step in simulation [s]
$\mathbf{u}$	gas velocity [m/s]
$\mathbf{v}_p$	particle velocity [m/s]
$\langle v \rangle_p$	time-averaged particle velocity [m/s]
V	volume [m^3]

X_w	moisture content [-]
$<X_w>$	averaged moisture load [-]

Greek letters

β	inter-phase momentum transfer coefficient [kg/(m^3 s)]
b_0	coefficient of tangential restitution [-]
ε	volume fraction [-]
λ_f	gas phase bulk viscosity [kg/(m s)]
m_f	gas phase shear viscosity [kg/(m s)]
m	dynamic friction coefficient [-]
r	density [kg/m^3]
t_f	gas phase stress tensor [Pa]
F	particle flux [kg/(m^{2}s)]
w	angular velocity [1/s]

Subscripts

bg	background fluidization
d	droplet
end	end of simulation
exp	experimental
f	fluid phase
mf	minimum fluidization
p	particle
pdf	pressure drop fluctuations
sim	simulation
sp	spout fluidization
sup	superficial
w	wall
x	horizontal direction
z	vertical direction
0	initial

INTRODUCTION

Spout fluidized beds are frequently used for the production of granules or particles through granulation, which are widely applied for example in the production of detergents, pharmaceuticals, food and fertilizers (Mörl et al., 2007). Spout fluidized beds have a number of advantageous properties, such as high mobility of the particles preventing undesired agglomeration and enabling excellent heat transfer control. The particle growth mechanism in a spout fluidized bed as function of the particle-droplet interaction has a profound influence on the particle morphology and thus on the product quality. During the granulation process, particles contain different loadings of moisture which results in varying collision properties in time and location across the bed. Consequently, the bed dynamics depend, amongst others, on collision properties. This has been shown by Passos & Mujumdar (2000) and Vieira & Rocha (2004), who experimentally investigated the flow behavior in spouted beds with dry respectively wet particles. They both observed a decrease of the particle velocity in the annulus with increasing moisture content, keeping constant all the operating conditions during a coating experiment. In addition, the bed pressure drop was found to decrease with increase of the instantaneous bed saturation degree. The stable spout pressure drop in the dry bed was found to be higher than that in the wet bed.

Fu et al. (2004) also studied the effect of the moisture content on collision properties experimentally. The collision properties between particles are captured in the restitution coefficient which is the ratio of the velocities associated with impact and rebound. They found that the restitution coefficient decreases with increasing moisture content, which they attributed to the reduction of the Young's modulus.

Mangwandi et al. (2007) experimentally investigated the impact behavior of three different types of granules, viz. wet, melt and binderless granules. Wet granules are defined as granules in which the primary particles are held together by liquid bridges; the melt granules are wet granules with solidified binder. They also found differences in restitution coefficients for the different types of granules.

Research has thus shown that the moisture content in spout fluidized beds has a great influence on the inter-particle collision properties and hence on the flow behavior.

It may therefore be concluded that a detailed description of the influence of the restitution coefficient on the bed dynamics is of great importance. However, such a description has not yet been obtained in detail due to the practical problems faced in the experimental study of spouted beds, such as infeasible non-intrusive access of the spout channel. Therefore, computational methods provide a powerful and attractive alternative for laborious experimental studies. In this work we use fundamental, deterministic models to enable the detailed investigation of granulation behavior in a spout fluidized bed. A discrete element model (DEM) is used, which describes the dynamics of the continuous gas-phase and the discrete particles and droplets. The model is based on the DEM originally developed by Hoomans et al. (1996) and extended by Link et al. (2007) for the simulation of spout fluidized beds. The DEM is further developed by improving the description of both the particle-droplet and particle-particle interactions. The effect of the moisture content on the particle-particle interaction is studied, by defining a relation between the restitution coefficient and moisture content. The objective of this work is to gain insight in the effect of the restitution coefficient on the flow behavior of spout fluidized beds at different flow regimes using the further developed DEM. The simulation results are compared with the simulation results of Van Buijtenen et al. (2007).

The organization of this paper is as follows: first, the DEM, including the improvement is briefly discussed. Then, the studied test cases are described and finally, the simulation results are discussed and compared with Van Buijtenen et al. (2007).

MODEL DESCRIPTION

The simulations are conducted with a discrete element model that describes the dynamics of the continuous gas-phase and the discrete particles and droplets. For each element force balances are solved. The momentum

transfer among each of the phases is described in detail at the level of individual elements. The inter-particle collisions are described using a soft sphere approach. In this approach, the particles are assumed to undergo deformation during their contact, where the contact forces are calculated from a simple mechanical analogue involving a spring, a dash-pot and a slider. This allows for energy dissipation due to non-ideal particle interaction by means of the empirical coefficients of normal and tangential restitution, and the coefficient of friction. In case a particle is in contact with several other particles the net contact force follows from the addition of all binary contributions. This approach was originally proposed by Cundall & Strack (1979) for granular matter. For further details on the collision model the interested reader is referred to the work of Hoomans et al. (1996) and Deen et al. (2007).

The motion of each individual particle present in the system is calculated from the Newtonian equation of motion:

$$m_p \frac{d\mathbf{v}_p}{dt} = -V_p \nabla p + \frac{V_p b}{\left(1-e_f\right)}\left(\mathbf{u}_f - \mathbf{v}_p\right) + m_p \mathbf{g} + \sum_{\forall b \in N_{part}} \mathbf{F}_{\mathbf{a}\leftrightarrow\mathbf{b}} + \sum_{\forall b \in N_{walls}} \mathbf{F}_{\mathbf{a}\leftrightarrow\mathbf{b}} \quad (1)$$

where β represents the inter-phase momentum transfer coefficient due to drag, which is calculated using a drag relation proposed by Koch & Hill (2001) based on lattice-Boltzmann simulations:

$$b_{Koch\&Hill} = \frac{18 m_f e_f^2 \left(1-e_f\right)}{d_p^2}\left(F_0\left(1-e_f\right) + \frac{1}{2}F_3\left(1-e_f\right)\mathrm{Re}_p\right) \quad (2)$$

The porosity is accounted for both particles and droplets, i.e. $e_f + e_p + e_d = 1$ and Re_p is given by:

$$\mathrm{Re}_p = \frac{e_f r_f \left|\mathbf{u}_f - \mathbf{v}_p\right| d_p}{m_f} \quad (3)$$

and with:

$$F_0\left(1-e_f\right) = \frac{1+3\sqrt{\frac{\left(1-e_f\right)}{2}} + \frac{135}{64}\left(1-e_f\right)\ln\left(1-e_f\right) + 16.1\left(1-e_f\right)}{1+0.68\left(1-e_f\right) - 8.48\left(1-e_f\right)^2 + 8.16\left(1-e_f\right)^3} \quad (4.1)$$

If $(1-\varepsilon_f) < 0.4$

$$F_0\left(1-e_f\right) = \frac{10\left(1-e_f\right)}{e_f^3} \quad (4.2)$$

If $(1-\varepsilon_f) \geq 0.4$

$$F_3\left(1-e_f\right) = 0.0673 + 0.212\left(1-e_f\right) + \frac{0.0232}{e_f^5} \quad (5)$$

The gas phase flow field is computed from the volume-averaged Navier-Stokes equations given by:

$$\frac{\partial}{\partial t}\left(e_f r_f\right) + \nabla \cdot \left(e_f r_f \mathbf{u}_f\right) = 0 \quad (6)$$

$$\frac{\partial}{\partial t}\left(e_f r_f \mathbf{u}_f\right) + \nabla \cdot \left(e_f r_f \mathbf{u}_f \mathbf{u}_f\right) = -e_f \nabla p - \nabla \cdot \left(e_f \mathrm{t}_f\right) - \mathbf{S}_p + e_f r_f \mathbf{g} \quad (7)$$

where the fluid density, ρ_f, is determined using the ideal gas law and the viscous stress tensor, t_f is assumed to obey the general form for a Newtonian fluid (Bird et al., 1960):

$$\boldsymbol{\tau}_f = -\left[\left(l_f - \frac{2}{3}m_f\right)\left(\nabla \cdot \mathbf{u}_f\right)\mathbf{I} + m_f\left(\left(\nabla \mathbf{u}_f\right) + \left(\nabla \mathbf{u}_f\right)^T\right)\right] \quad (8)$$

Turbulence is not accounted for, as it is entirely dampened by the presence of the particles.

Two-way coupling is achieved via the sink term, $\mathbf{S}_p$, which is computed from:

$$\mathbf{S}_p = \frac{1}{V_{cell}} \sum_{\forall i \in cell} \frac{V_i b}{\left(1-e_f\right)}\left(\mathbf{u}_f - \mathbf{v}_i\right) D\left(\mathbf{r} - \mathbf{r}_i\right) \quad (9)$$

The distribution function, *D*, distributes the reaction force acting on the gas phase to the velocity nodes in the staggered Eulerian grid.

Description of droplets

The DEM extended by Link et al. (2007) contains a simplified description of the phenomena in which the droplets are involved. In this work the DEM is improved by incorporating the equation of motion of the droplets and the two-way coupling of the drag between the droplets and the gas phase. The equation of motion resembles that of the particles, although it is assumed that the droplets do not collide with each other, because of their small size and low volume fraction:

$$m_d \frac{d\mathbf{v}_d}{dt} = -V_d \nabla p + \frac{V_d b}{\left(1-e_f\right)}\left(\mathbf{u}_f - \mathbf{v}_d\right) + m_d \mathbf{g} \quad (10)$$

The inter-phase momentum transfer coefficient due to drag is calculated in the same way as for the particles (Eq. 2), using the Reynolds number for the relative velocity of the droplets and the droplet size.

Particle-droplet interaction

Since the impact of an individual encounter between a droplet and a particle is small, the interaction between droplet and particle is described differently compared to particle-particle collisions. When the droplet meets a particle, it transfers its mass and momentum to the particle and disappears.

The particle growth can therefore be defined as an addition of the mass of the droplet, and the velocity of the particle is affected by momentum transfer of the droplet:

$$m'_p = m_p + m_d \quad (11)$$

$$\mathbf{v}'_p = \frac{\mathbf{v}_p m_p + \mathbf{v}_d m_d}{m'_p} \quad (12)$$

Furthermore, it is assumed that the angular velocity is unaffected by the particle-droplet interaction:

$$w'_p = w_p \quad (13)$$

The resulting particle remains spherical and the position of the particle is not altered:

$$\mathbf{r}'_p = \mathbf{r}_p \quad (14)$$

The diameter of the particle increases:

$$d'_p = \left(d_p^3 + d_d^3\right)^{1/3} \quad (15)$$

Due to the droplet-particle interactions, a particle consists of an amount of moisture, which is defined as the moisture content:

$$X_w = \frac{\sum_{N_{coll,p\leftrightarrow d}} m_d}{m'_p} \tag{16}$$

The mass of moisture is formulated as the summation of the mass of each droplet hitting the relevant particle.

Particle-particle interaction

The interaction between particles is affected by the moisture content, since the particles collide less ideal with increasing moisture load. This is approximated with the following relation:

$$e_{n,p} = \left(e_{n,p_0} - e_{n,p_{sat}}\right)\cdot 10^{-5X_w} + e_{n,p_{sat}} \qquad (17)$$

Where $e_{n,p0}$ is the normal restitution coefficient of the dry particle, i.e. X_w = 0, and $e_{n,psat}$ is the normal restitution coefficient of a saturated particle.

This relation is based on detailed impact measurements (Vorhauer, 2007) of dry particles on a flat plate with a thin liquid layer. When two particles (a and b) with different restitution coefficients collide, an 'overall restitution coefficient' is determined using harmonic averaging:

$$e^{-1}_{n,p,ab} = \frac{1}{2}\left(e^{-1}_{n,p,a} + e^{-1}_{n,p,b}\right) \qquad (18)$$

TEST CASES

The objective of this work is to study the bed dynamics as a function of the restitution coefficient, which varies in time and space due to the particle-droplet interaction.

To this end, several simulations have been conducted for different flow regimes, which are chosen in accordance with the simulations of Van Buijtenen et al. (2007). To enable the study of a variable restitution coefficient, the growth of the particle is neglected in this work. That is, the particle mass and volume remain constant (Eqs. 11 and 15), while only the restitution coefficient changes with varying moisture content. Subsequently, the geometry of the 3D spout-fluidized bed and the numerical settings comply with the previously conducted simulations.

Van Buijtenen et al. (2007) simulated different cases in which the restitution coefficient ranges from 0.2 to 0.97, being constant in time and location across the bed.

Tables 1 and 2 respectively list the properties of the particles and the droplets. The density of the droplets is somewhat arbitrarily chosen to be the same as that of the particles. The studied flow regimes are shown in Table 3, whereas the numerical settings are listed in Table 4 (for further details of the numerical procedure, the interested reader is referred to Hoomans et al., 1996). The schematic representation of the geometry of the 3D spout fluidized bed is displayed in Figure 1.

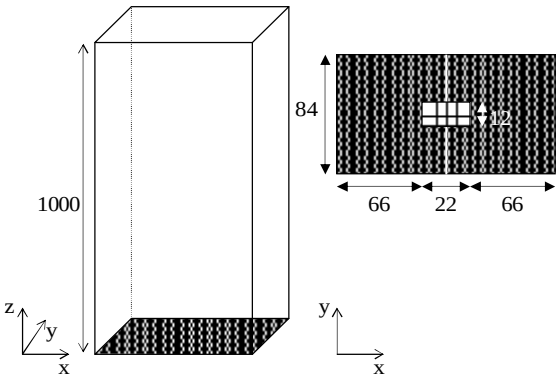

Figure 1: Schematic representation of the geometry of the 3D spout fluidized bed, dimensions are given in mm.

Table 1: Particle properties.

Property	Value	Unit
Material	Glass	n.a.
d_p	4.0	mm
r_p	2526	kg/m^3
$e_{n,p\leftrightarrow p,0}$	0.97	-
$e_{n,\,p\leftrightarrow w,0}$	0.97	-
$e_{n,p\leftrightarrow p,sat}$	0.10	-
$e_{n,p\leftrightarrow w,sat}$	0.10	-
$m_{\,p\leftrightarrow p}$	0.10	-
$m_{\,p\leftrightarrow w}$	0.10	-
$b_{0\,,p\leftrightarrow p}$	0.33	-
$b_{0,p\leftrightarrow w}$	0.33	-

Table 2: Droplet properties.

Property	Value	Unit
d_d	0.4	mm
r_d	2526	kg/m^3
m_d	$8.465\cdot10^{-8}$	kg

Table 3: Flow regimes.

Case	Flow regime	u_{bg}		u_{sp}		u_{sup}	
		[m/s]	[u_{mf}]	[m/s]	[u_{mf}]	[m/s]	[u_{mf}]
B1	Intermediate / Spout-fluidization	2.5	1.4	60	34	3.7	2.1
B2	Spouting-with-aeration	2.5	1.4	90	51	4.3	2.4
B3	Jet-in-fluidized-bed	3.5	2.0	65	37	4.8	2.7

Table 4: Numerical settings.

Property	Value	Unit
N_x	21	-
N_y	14	-
N_z	100	-
t_{sim}	10	s
Δt	$5\cdot10^{-5}$	s
N_p	$4.48\cdot10^4$	-
k_n	10^4	N/m
$\dot{N}_{drop}$	$8.5\cdot10^5$	drops/s

RESULTS AND DISCUSSIONS

To study the effect of the variable restitution coefficient on the bed dynamics, the following aspects will be examined:

- Bed height
- Pressure drop
- Particle velocity

The bed height and pressure drop are presented to study the overall bed dynamics, and the particle velocity to capture more details of the particle motion in the bed as function of the restitution coefficient. The bed height is defined as the averaged z-location of the particles:

$$< r_z >= \frac{1}{N_{part}} \sum_{N_{part}} r_z \qquad (19)$$

The results reported by Van Buijtenen et al. (2007) are included to enable a comparison between a constant restitution coefficient and a moisture content dependent restitution coefficient. An overall restitution coefficient is determined by calculating the average moisture load under the assumption that the added moisture is equally distributed over the particles:

$$\langle X_w \rangle = \frac{F_{drop} r_d V_d t}{N_{part} r_p V_p} \tag{20}$$

The overall restitution coefficient $<e_n>$ is then calculated using Eq. (17). Time t is chosen in such a way that the overall restitution coefficient complies with those from the previously conducted simulations, i.e. from $e_n = 0.8$ down to 0.2, distinguishing the different stages of the wetting process (see Figure 2).

Snapshots of the simulated instantaneous particle positions of both the constant and variable restitution coefficient are presented in Figure 3, showing the bed behaviour for different restitution coefficients for the three cases.

The time-averaged distribution of the restitution coefficient is displayed in Figure 4 for every stage of the wetting.

Below, the results of the bed height and the pressure drop will be shown, followed by a presentation of the particle velocity profiles.

Bed height and pressure drop

In Figure 5 and Figure 6 the time-averaged bed height and pressure drop are shown respectively. Note that the bed height and pressure drop corresponding to the previous results is averaged over a period of 10 s, whereas the bed height and pressure drop of the wetting process simulation are averaged over approximately 1.5 s. This period is chosen to gain a time-averaged restitution coefficient which deviates ±5% around the constant value. Note that due to the short averaging period, the time-averaged bed height and pressure drop will have larger uncertainties.

In the simulations with constant restitution coefficient, the first 10 s were excluded from the spectral analysis to prevent start-up effects from influencing the results. The wetting process simulations were initiated at the end of the simulations with $e_n = 0.97$, injecting droplets in a spout-fluidized bed in which realistic bed dynamics prevails. In Figure 3 therefore the instantaneous snapshots of the simulation with constant $e_n = 0.97$ is displayed as a reference. It is found that the average bed height decreases with increasing restitution coefficient for both the constant and variable restitution coefficient. This is due to decreasing bubble hold-up. Particles with low restitution coefficient tend to promote the formation of dense regions and passage of gas through the bed mainly occurs in the form of bubbles.

Furthermore, for the variable restitution coefficient the bed height comprises a higher value for every restitution coefficient and flow regime. This may be due to the fact that during the granulation process, the particles in the spout region contain the highest moisture content and thus the lowest restitution coefficient (see Figure 4). These particles tend to cluster and as a result are dragged higher up in the bed.

The influence of the restitution coefficient on the pressure drop exhibits a different trend than that of the bed height. Apparently, contrary to conventional fluidized beds, for spout fluidized beds the pressure drop is not inversely proportional to the bed height. This may be due to the heterogeneity prevailing in spout fluidized beds, i.e. the presence of a core-annulus structure. Although, no similar influence of the restitution coefficient on the pressure drop can be observed, the value of the pressure drop is lower for all the simulations with variable restitution coefficient. This does comply with the trends observed at the bed height.

Particle velocity

Time-averaged velocity fields were obtained over a short period of time as to ensure an approximately constant distribution of the restitution coefficient. This period is chosen in such a way that the overall restitution coefficient had a deviation of maximal ±5% around the constant restitution coefficients. In the simulations with the constant restitution coefficient longer averaging periods were used to obtain statistically justified results. The time averaged velocities were calculated by averaging over all particles, employing the same numerical grid that is used to solve the gas phase dynamics:

$$\langle \mathbf{v}_{i,j,k} \rangle = \frac{\sum_{t=t_0}^{t_{end}} \sum_{p=1}^{N_p} \mathbf{v}_p(t) d}{\sum_{t=t_0}^{t_{end}} \sum_{p=1}^{N_p} d} \quad \forall d = \begin{cases} 1 & \forall p \in (i,j,k) \\ 0 & \forall p \notin (i,j,k) \end{cases}, \tag{21}$$

where p represents a particle in cell (i, j, k). N_p is the number of particles, and t_0 and t_{end} are respectively the start and end times of the averaging period.

Particle velocity profiles at a height z = 0.15 m in the central xz-plane are shown in Figure 7 illustrating the particle velocities in the annulus and the spout channel, for all the variable and constant restitution coefficients and the three cases. Figure 8 displays the time-averaged particle velocity for $<e_n> = 0.4$ and $e_n = 0.4$ for case B2 and B3. It can be seen that the particle velocity in the spout region increases with decreasing restitution coefficient especially for the variable restitution coefficient for case B1 and B2. Furthermore, the particle velocity in the spout region for the variable restitution coefficient is lower than the constant restitution coefficient. This may be due to the fact that for the variable restitution coefficient, the particles in the annulus contain a higher restitution coefficient as shown in Figure 4, since they have not yet been exposed to the droplet beam.

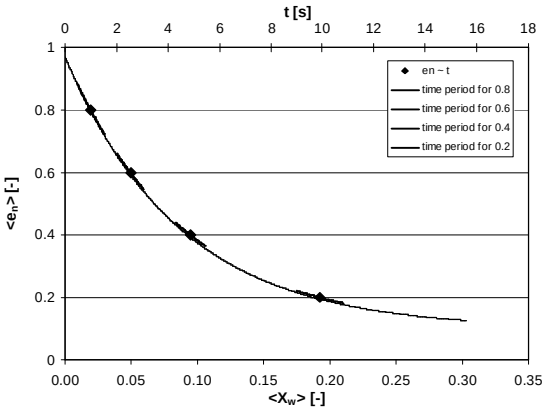

Figure 2: Overall restitution coefficient versus time and average moisture load. The chosen time-period per stage of the granulation or wetting process is visualized.

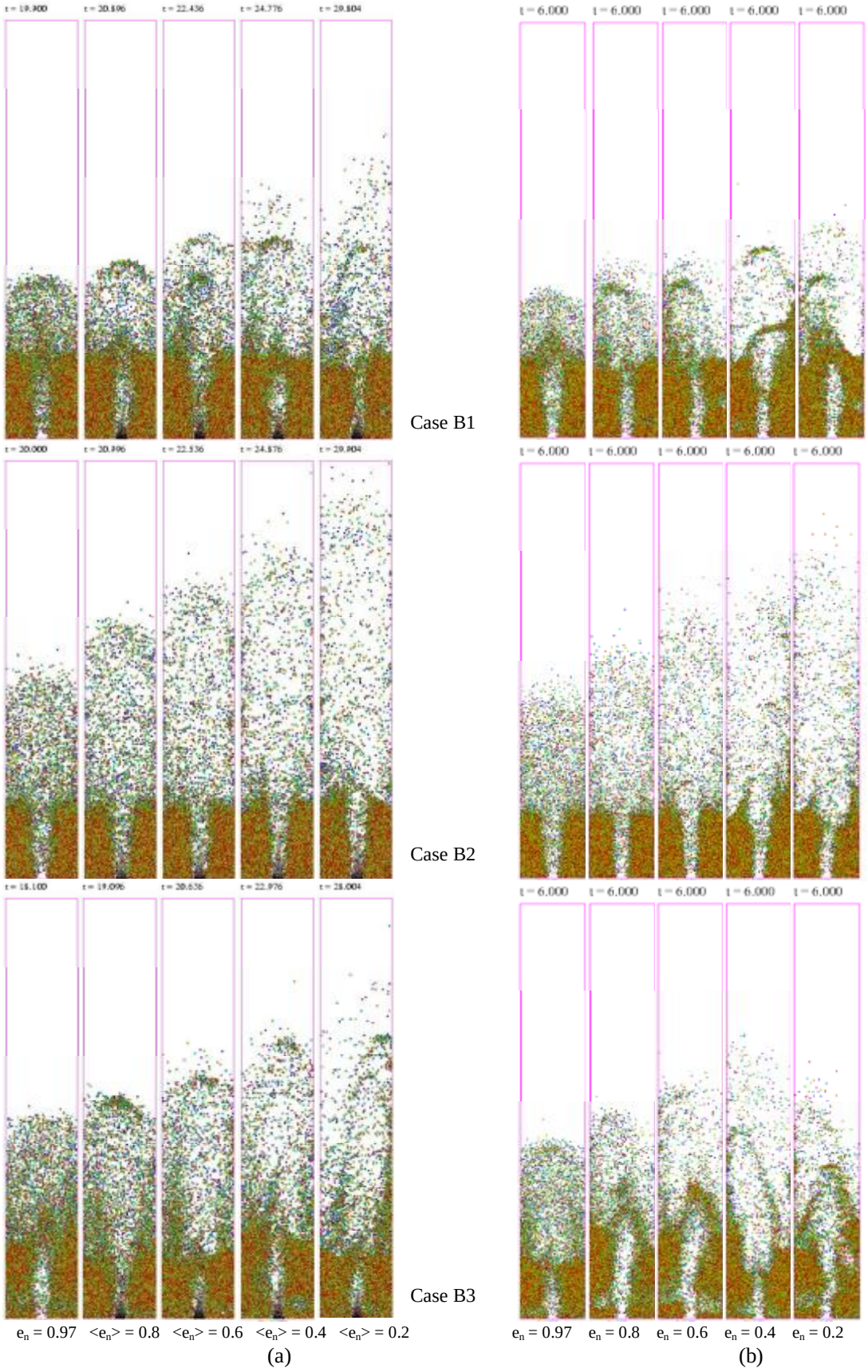

Figure 3: Snapshots of the simulated instantaneous particle positions for different variable restitution coefficients (a) at different stages of the wetting process distinguished by the overall restitution coefficient <e_n> and different constant restitution coefficients (b) at simulation time t = 6 s for case B1 (intermediate / spout - fluidization regime), B2 (spouting-with-aeration regime) and B3 (jet-in-fluidized-bed regime).

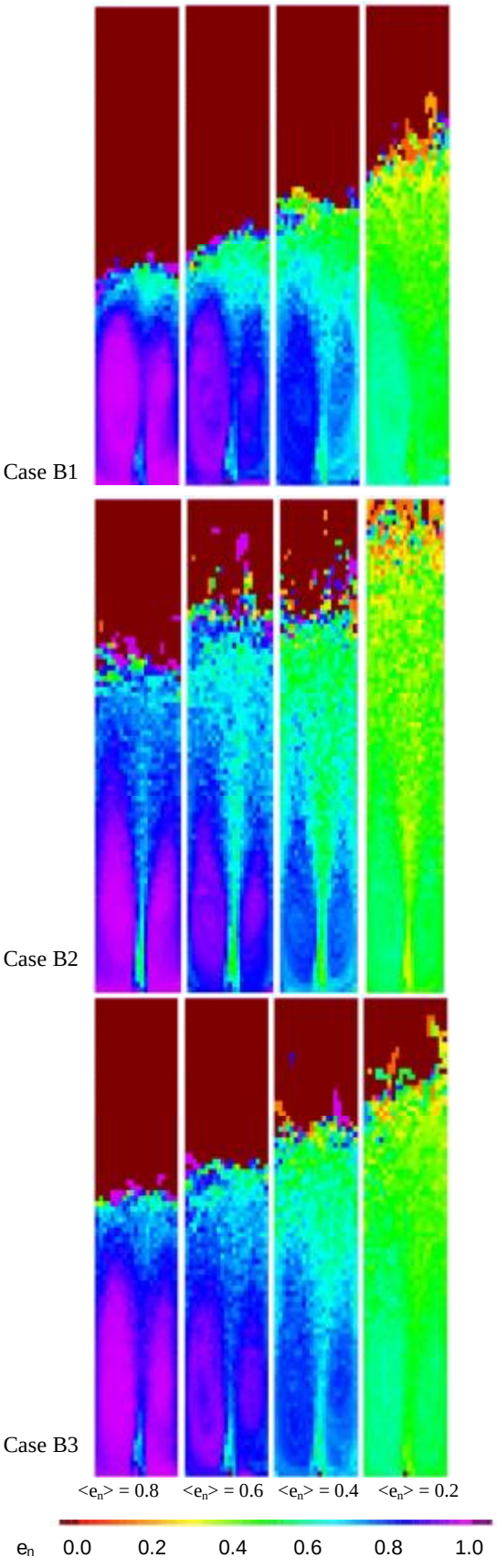

Figure 4: Time-averaged restitution coefficient per grid cell for different variable restitution coefficients for case B1 (intermediate / spout - fluidization regime), B2 (spouting-with-aeration regime) and B3 (jet-in-fluidized-bed regime) at different stages of the wetting process, distinguished by the overall restitution coefficient <e_n>.

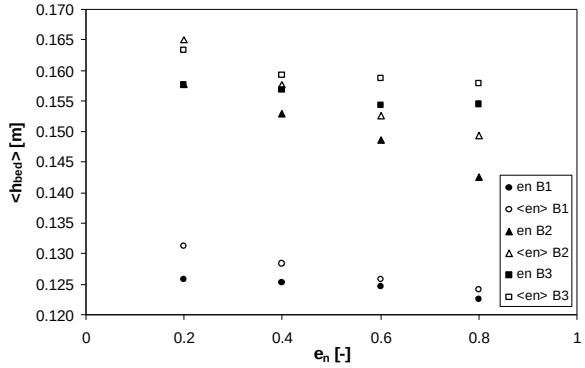

Figure 5: Time-averaged bed height for different constant restitution coefficients (e_n as reported in Van Buijtenen et al. (2007)) and different variable restitution coefficients at different stages of the wetting process, distinguished by the overall restitution coefficient <e_n>, for case B1 (intermediate / spout - fluidization regime), B2 (spouting-with-aeration regime) and B3 (jet-in-fluidized-bed regime).

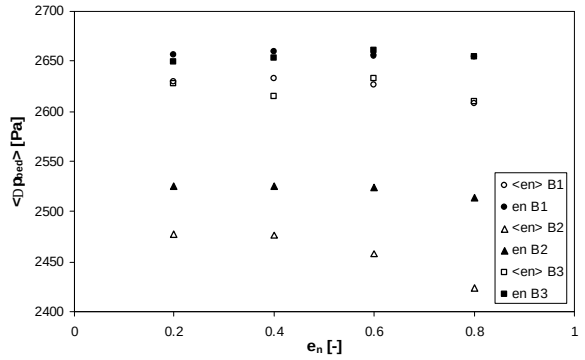

Figure 6: Time-averaged pressure drop for different constant restitution coefficients (e_n as reported in Van Buijtenen et al. (2007)) and different variable restitution coefficients at different stages of the wetting process, distinguished by the overall restitution coefficient <e_n>, for case B1 (intermediate / spout - fluidization regime), B2 (spouting-with-aeration regime) and B3 (jet-in-fluidized-bed regime).

As a result, the formation of dense regions in the annulus is less pronounced compared to the constant restitution coefficient case. Consequently more gas will move through the annulus, leading to a somewhat lower gas and particle velocities in the spout region.
However, for case B3, the particle velocity for the variable restitution coefficient complies with the constant restitution coefficient. In Figure 8 the particle velocity for case B3 and B2 for the variable restitution coefficient is compared to the constant restitution coefficient. It can be seen clearly that the particle velocity for the variable restitution coefficient is lower than for the constant restitution coefficient for case B2, whereas for case B3 they comply. The interaction between the spout channel and the bubbles present in the annulus is larger for case B3 than for case B2, as more bubbles are present in the former case. Better mixing of the particles happens by which fewer regions are present containing large differences in restitution coefficient. This is clearly seen in Figure 4, for <e_n> =

0.4 and 0.2, where the colour differences are less pronounced than for case B3.

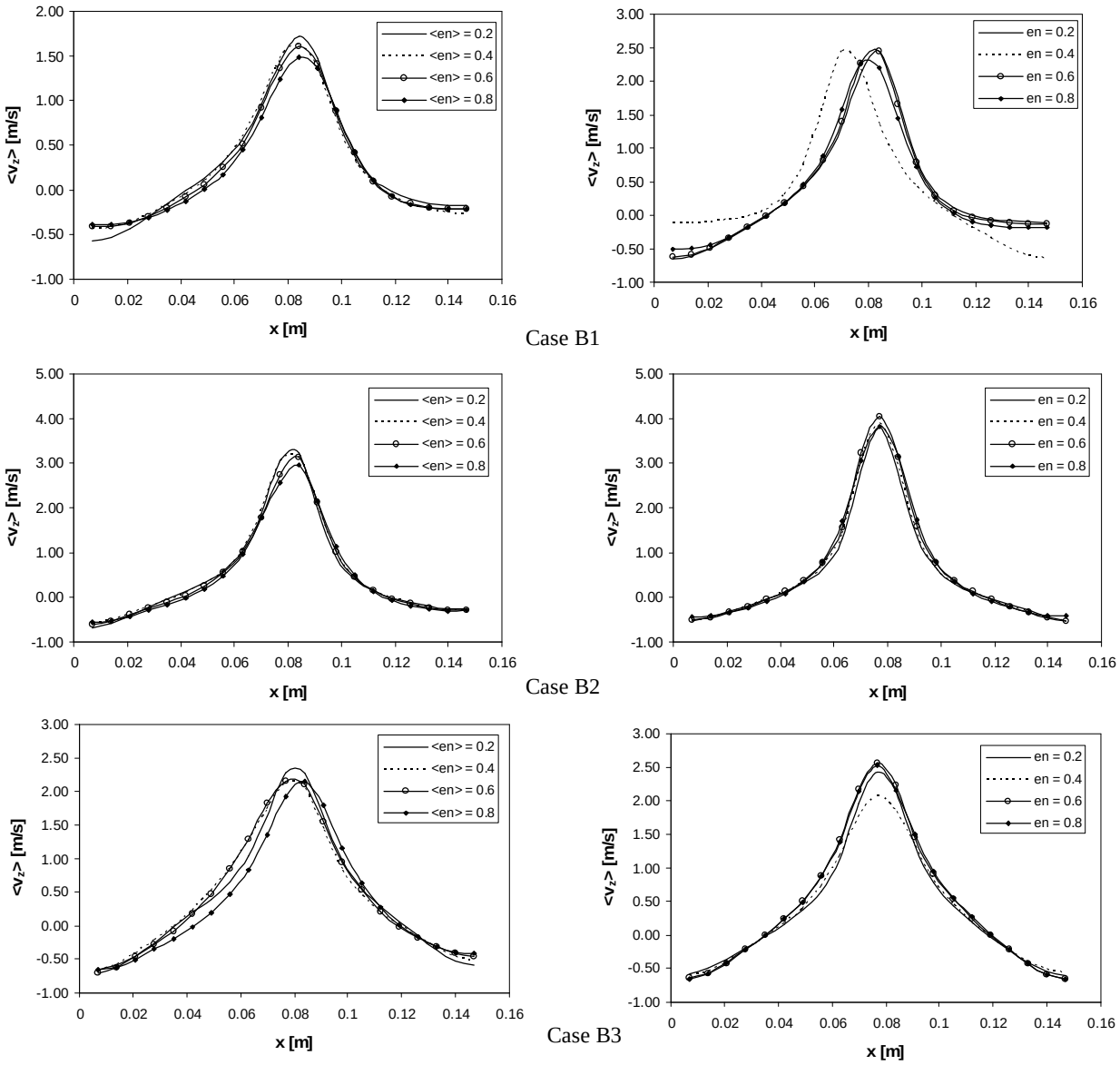

Figure 7: Profiles of the time-averaged vertical particle velocity for different variable (a) and constant (a) restitution coefficients at z = 0.15 for case B1 (the intermediate /spout-fluidization regime), B2 (spouting-with-aeration regime) and B3 (jet-in-fluidized-bed regime).

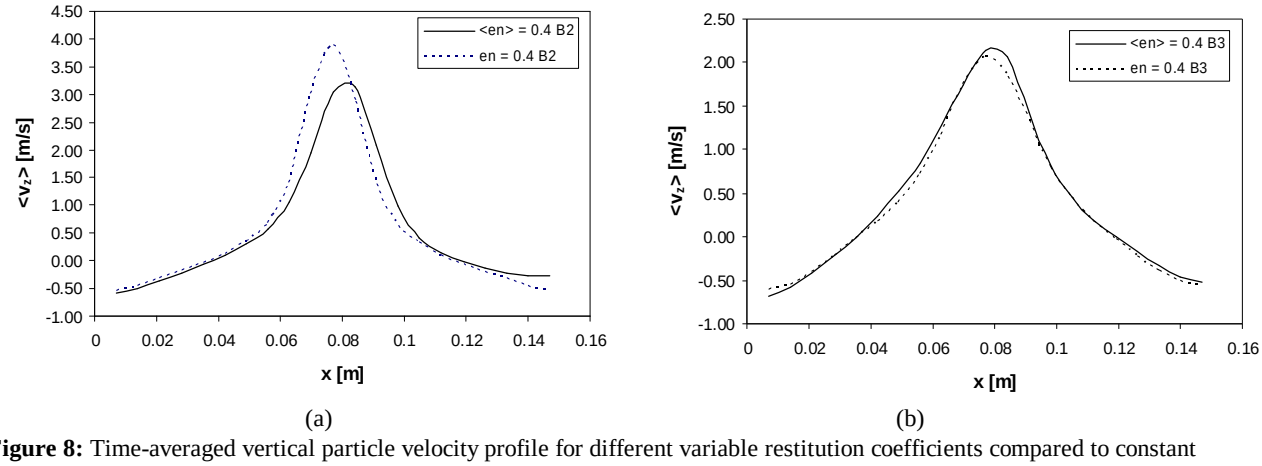

Figure 8: Time-averaged vertical particle velocity profile for different variable restitution coefficients compared to constant restitution coefficients for case B2, the spouting-with-aeration regime (a) and case B3, jet-in-fluidized-bed regime (b) at z = 0.15.

CONCLUSIONS

In this paper the influence of the restitution coefficient on the bed dynamics is studied using the discrete element model (DEM), where the restitution coefficient is time and space dependent due to the particle-droplet interaction. The bed height, bed pressure drop, and the time-averaged vertical particle velocity were determined. For our study three flow regimes were investigated: the intermediate / spout-fluidization regime (B1), spouting-with- aeration regime (B2) and the jet-in-fluidized-bed regime (B3). The simulation results with variable restitution coefficients were compared to simulations with constant restitution coefficients reported by Van Buijtenen et al. (2007). The increasing trend in the average bed height with decreasing restitution coefficient is also valid for the variable restitution coefficient. However, the average bed height is larger for the variable restitution coefficient for all flow regimes. This is also observed for the pressure drop, showing a lower value compared to the constant restitution coefficient.

These results suggest a significant influence of the variable restitution coefficient on the bed dynamics, since the variable restitution coefficient provides regions in the bed with particles having different collision properties. The presence of these distinctive regions causes different behavior of the bed dynamics, which is also displayed in the time-averaged vertical particle velocity. First, the velocity in the spout region for the variable restitution coefficient is lower than for the constant restitution coefficient for case B1 and B2. In these cases, the regions with different restitution coefficient are clearly seen in Figure 4. Second, for case B3, the particle velocity for the variable and constant restitution coefficient comply, which can be explained by the larger mixing capacity caused by the larger interaction between the spout channel and bubbles in the annulus region. In Figure 4 the regions with different restitution coefficients are less distinctive for this case.

These findings reveal the significant impact of the influence of the variable restitution coefficient on the dynamics of the bed, which is clearly different compared to the constant restitution coefficient. This is due to the presence of distinctive regions with different restitution coefficient, which can only be simulated when the dependency of the moisture content on the restitution coefficient is accounted for.

Currently, only the wetting process on the particles has been simulated without evaporation and crystallization of the deposited granulate solution, which are phenomena that are very important in the granulation process. It is therefore desirable to further improve the discrete element model, by solving mass and energy balances for the particles and the gas phase.

ACKNOWLEDGEMENTS

The authors would like to thank FOM, STW and Yara Sluiskil, The Netherlands, for their financial support to the project.

REFERENCES

BIRD, R.B., STEWART, W.E., LIGHTFOOT, E.N.,(1960), “Transport phenomena”, New York: John Wiley & Sons, 79.

BUIJTENEN VAN, M.S., DEEN, N.G., HEINRICH, S., ANTONYUK, S., KUIPERS, J.A.M., (2007), “Improvement of the discrete element model for the study of granulation in a spout fluidized bed”, *6th Int. Conf. Multiphase Flow*, ICMF 2007, Leipzig, Germany, July 9 – 13, 2007, paper no. 266.

CUNDALL, P.A, & STRACK, O.D., (1979), ”A discrete numerical model for granular assemblies.” *Geotechnique*, 29, 47-65.

DEEN, N.G., VAN SINT ANNALAND, M., VAN DER HOEF, M.A., KUIPERS, J.A.M., (2007), “Review of discrete particle modeling of fluidized beds.”, *Chem. Eng. Sci.*, 62, 28-44.

FU, J., ADAMS, M.J., REYNOLDS, G..K., SALMAN, A.D., HOUNSLOW, M.J., (2004), “Impact deformation and rebound of wet granules.” *Powder Technol.*, 140, 248-257.

HOOMANS, B.P.B., KUIPERS, J.A.M., BRIELS,, W.J., VAN SWAAIJ, W.P.M., (1996), “Discrete particle simulation of bubble and slug formation in a two-dimensional gas-fluidised bed: a hard-sphere approach.” *Chem. Eng. Sci*, 51, 99-118.

KOCH, D.L. & HILL, R.J., (2001), ”Inertial effects in suspension and porous-media flows.”, *Ann. Rev. Fluid Mech.*, 33, 619-647.

LINK., J.M., CUYPERS, L.A., DEEN, N.G., KUIPERS, J.A.M., (2005), “Flow regimes in a spout-fluid bed: A combined experimental and simulation study.”, *Chem. Eng. Sci.*, 60, 3425-3442.

LINK, J.M., GODLIEB, W., DEEN, N.G., KUIPERS, J.A.M., (2007), “Discrete element study of granulation in a spout-fluidized bed.”, *Chem. Eng. Sci.*, 62, 195-207.

LINK, J.M., (2006), “Development and validation of a discrete particle model of a spout-fluid bed granulator.”, *Ph.D. Thesis*, Univ. of Twente, The Netherlands, p. 90.

MANGWANDI, C., CHEONG, Y.S., ADAMS, M.J., HOUNSLOW, M.J., SALMAN, A.D., (2007), “The coefficient of restitution of different representative types of granules.”, *Chem. Eng. Sci.*, 62, 437-450.

MÖRL, L., HEINRICH, S., PEGLOW, M. (Eds.: SALMAN, A., HOUNSLOW, M., SEVILLE, J.P.K., (2007), “Fluidized bed spray granulation”, Granulation (Handbook of Powder Technology, Volume 11), Chapter: The Macro Scale I: Processing for Granulation, Elsevier Science, 21-188, ISBN 0-444-51871-1.

PASSOS, M.L. & MUJUMDAR, A.S., (2000), “Effect of cohesive forces on fluidized and spouted beds of wet particles.”, *Powder Technol.*, 110, 222-238.

VIEIRA, M.G.A. & ROCHA, S.C.S., (2004), “Influence of the liquid saturation degree on the fluid dynamics of a spouted-bed coater.”, *Chem. Eng. Proc.*, 43, 1275-1280.

VORHAUER, N., (2007), "Untersuchung des Einflusses von Flüssigkeitsschichten auf das Stoβverhalten elastisch-plastischer Granulate", ***Master Thesis***, Otto-von-Guericke-University Magdeburg, Germany, p. 87